

Laser transmission welding of Acrylonitrile-Butadiene-Styrene (ABS) using a tailored high power diode-laser optical fiber coupled system

E.Rodríguez-Vidal^{*a}, I.Quintana^a, J.Etxarri^a, D.Otaduy^a, F.González^b, and F.Moreno^b

^aFundación Tekniker, Avda. Otaola, 20, 20600 Eibar, Guipúzcoa, Spain

^bGroup of Optics, Applied Physics Department, University of Cantabria, Avda. de los Castros, s/n 39005, Santander, Spain.

ABSTRACT

Laser transmission welding (LTW) of polymers is a direct bonding technique which is already used in different industrial applications sectors such as automobile, microfluidic, electronic and biomedicine. This technique offers several advantages over conventional methods, especially when a local deposition of energy and minimum thermal distortions are required. In LTW one of the polymeric materials needs to be transparent to the laser wavelength and the second part needs to be designed to be absorbed in IR spectrum. This report presents a study of laser weldability of ABS (acrylonitrile/butadiene/styrene) filled with two different concentrations of carbon nanotubes (0.01% and 0.05% CNTs). These additives are used as infrared absorbing components in the laser welding process, affecting the thermal and optical properties of the material and, hence, the final quality of the weld seam.

A tailored laser system has been designed to obtain high quality weld seams with widths between 0.4 and 1.0mm. It consists of two diode laser bars (50W per bar) coupled into an optical fiber using a non-imaging solution: equalization of the beam quality factor (M^2) in the slow and fast axes by a pair of micro step-mirrors. The beam quality factor has been analyzed at different laser powers with the aim to guarantee a coupling efficiency to the multimode optical fiber. The power scaling is carried out by means of multiplexing polarization technique. The analysis of energy balance and beam quality is performed in two linked steps: first by means ray tracing simulations (ZEMAX[®]) and second, by validation.

Quality of the weld seams is analyzed in terms of the process parameters (welding speed, laser power and clamping pressure) by visual and optical microscope inspections. The optimum laser power range for three different welding speeds is determinate meanwhile the clamping pressure is held constant. Additionally, the corresponding mechanical shear tests were carried out to analyze the mechanical properties of the weld seams. This work provides a detailed study concerning the effect of the material microstructure and laser beam quality on the final weld formation and surface integrity.

Keywords: laser transmission welding, polymer, carbon nanotubes, high power diode laser bars, beam quality, optical design, polarization multiplexing.

1. INTRODUCTION

Over the past few years, plastic welding techniques have attracted a considerable interest from a number of different industrial sectors such as automotive, packaging and healthcare [1-6]. Depending on the application and technical requirements of the component, joining of thermoplastics can be divided into mechanical fastening, adhesive and fusion bonding [1, 7- 9]. Laser transmission welding (LTW) belongs to the last category and it is usually used in applications where the hermetic adhesion and the minimization of the surrounding affected area are critical requirements [5, 8, 10-13]. LTW evolves localized heating at the interface of two pieces of plastic to be joined. One of the plastics needs to be optically transparent to the laser radiation whereas the other part has to be absorbent. The laser energy that is absorbed in this material causes vibration of electron bonds, followed by heat transfer to the surroundings through convection and radiation. When heated to temperatures above the melting point (or glass transition temperature in the case of amorphous polymers), the thermoplastic begins to flow and a weld is formed while applying a pressure to increase mating contact forces. The molten plastic improves the heat contact between both parts and involves an internal joining pressure to build

up through volume expansion. Depending on the optical and thermal properties of the absorbed part, the incident radiation is absorbed over a certain depth of the bottom material [14-16].

CO₂ Laser systems ($\lambda=10.6\text{mm}$) have been traditionally used in welding applications of thin plastic films, as a consequence of the high absorption coefficient of these material to medium infrared radiation [8,16-18]. The radiation produced by diode laser, however, is less readily absorbed by plastics and, together with the fact that these systems show high electro-optical efficiency, make them a very good alternative for plastic laser transmission welding. Their application on a given material can be done either directly from the diode laser bars or by means of a fiber optics arrangement.[18]. In this particular case, the laser-fiber coupling is not straightforward since the radiation emitted from HPDL (High Power Diode Lasers) bars suffers from two asymmetries: astigmatism and an elliptical beam profile. The divergence angles are different in the two axes, so-called "fast-axis" and "slow-axis". The emerging laser beam is a stripe with different beam profiles in both directions [19-21]. Different approaches have been proposed to shape the diode laser emission to obtain a circular focus spot. *Zbinden et al. and Graf et al.* [22-23] considered a diode laser bar are coupled into a multitude of fibers leading to a fiber bundle at the output end. *Yamaguchi et al.* [24] considered a multiprism array leading to a short dotted lines arrangement in parallel direction. *Clarkson et al.* [25] considered two plane parallel mirrors to reshape the emission from diode laser bars. Finally *Ehlers et al. and Treush et al.* [20, 26] employed step-mirrors to rearrange the emission from the diode laser bars and to couple it into an optical fiber. The later is currently a well-known and efficient technique with easy alignment requirements and low manufacturing costs.

To increase the output power compared with a single diode laser bar, the emission of multiple diode laser bars has to be combined. Incoherent beam combination of individual diode laser bars is presently widely used in laser systems for material processing. The basic techniques used, which increase output power at constant beam size are: wavelength and polarization multiplexing [20; 27].

In the present work, a tailored laser system with a maximum output power 67W has been designed by ZEMAX[®] optical design software. The system consists of a pair of step-mirrors for beam shaping. The modular design permits power scaling using polarization multiplexing technique. The beam quality factor was analyzed to guarantee a coupling efficiency to two optical fibers ($\Phi=600/400\mu\text{m}$, NA=0.22). Laser transmission welding of ABS was performed by the laser system described in this work. Quality of weld seams was analyzed in terms of process parameters by optical microscope inspection. In addition to this, the corresponding mechanical shear tests were carried out to characterize the mechanical properties of the weld seams.

2. MATERIALS AND METHODS

The polymer employed in this work was BASF Terluran[®] GP-35 ABS (ABS), a complex mixture consisting of styrene-acrylonitrile copolymer, a graft polymer of styrene-acrylonitrile and polybutadiene and some unchanged polybutadiene rubber [28]. The experimental investigation involved two types of ABS plates: the first component is a natural ABS, semitransparent to the infrared laser radiation, and the second one is a doped ABS (Nanocyl 700 CNTs) with different weight percent of carbon nanotubes: 0.01 and 0.05 %. The additive polymers were prepared starting from a high concentration of carbon nanotubes and subsequently, dissolution was performed in order to achieve the desired low concentration of carbon nanotubes (masterbatch). Due to this addition of the base polymer, both thermal and optical properties of the polymer would change significantly, affecting the final quality of the weld seam.

The laser beam from the presented laser system (optical fiber $\Phi=600\mu\text{m}$, NA=0.22) was focused over the sample by focusing lens placed in air with a 50 mm focal length. Spot size (beam diameter at $1/e^2$) of $w_0 = 976.2 \pm 0.4\mu\text{m}$ was obtained at laser power emission of 8W. Sample position can be selected with lateral resolution of 1mm and a depth control of roughly $10\mu\text{m}$, through a machining table with X/Y axes and Z positioning system.

The main process parameters affecting the bond quality are: the laser power, the welding speed and time, the laser beam size and uniformity, the optical properties of the polymeric material at the interface and the clamping pressure. Consequently, laser transmission welding experiments involving natural and partially doped ABS was carried out by changing laser parameters, such as speed and incident power. Three different welding speeds were considered: 10mm/s, 15mm/s and 20mm/s, allowing us to determine the explicit relationship between laser power and welding speed, while holding all other variables are constant. Contour welding experiments were performed by focusing the laser beam on the back face (partially doped ABS) and moving it over the welding contour. In this configuration, welded joints were

obtained by joining two rectangular polymer sheets, partially overlapped for a length of 35 mm and a surface of 40x45 mm². A clamping device for flat plates ensures uniform clamping pressure of 1N.m along the weld seam (figure 1). Weld seam widths were measured using optical microscopy [Olympus SZX16 U-TV0.5xC-3]. Micrographs were taken of the weld surface, through the transparent part about 10 mm from the starting point of the weld. Material decomposition, degradation, melting zone and porosity of the weld was estimated by microscopic examination of a polished cross – section of the welded material. The cross section specimens of microscopic examination were taken in the middle of the weld seam.

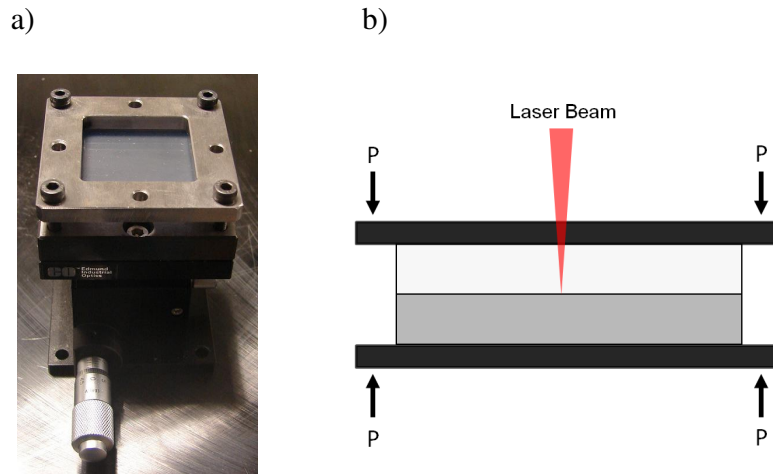


Figure 1. a) Experimental and b) schematic set-up for laser welding of ABS plates. Bottom part: ABS with additives (CNT), top part: ABS without filled.

Mechanical testing of welded plastic joints were carried out in an INStron 3369 Static Universal Testing machine [SN3369k2004] with a maximum load capacity of 50kN and a cross – head displacement rate of 5 mm/min according with ASTM D638-82a “Standard Test Method for Tensile properties of plastics”. Samples with rectangular geometry (23 x 80 mm² and 1 mm thickness) were prepared considering a gauge length of 40 mm and a weld seam location centered on the gauge length. For each irradiation dose, three specimens were tested and the maximum load reached during the tensile tests (N) was recorded until failure.

3. OPTICAL DESIGN

The diode laser bars are linear arrangement of large area emitters of incoherent radiation characterized by an astigmatism and elliptical beam profile. In this paper, double sided micro – optical arrays are used for fast axis (FAC) and slow axis (SAC) collimation, reducing the asymmetric divergence and improving the beam quality [27]. The laser sources considered are two similar diode laser bars from Jenoptik Laser GmbH. Each bar consists of 19 broad area emitters (collimation in both axes (FAC<0.5°, SAC<4°) and 30% Fill Factor) with a maximum output power per bar of about 50W CW at $\lambda=808\pm 4\text{nm}$: JOLD-50-CPBN-1L [29].

The beam quality of a diode laser bar is usually quantified by the Beam Parameter Product* (BPP), defined as a product of the beam waist and the beam divergence at half angle in the far field. The BPP in slow axis direction depends on the number of emitters and the spaces between them [30-31]. A ‘diagonal’ BPP to combine fast and slow axis and to compare with the rotationally symmetric BPP of the optical fiber is widely defined by Eq.(1) [32].

* Defined as $BPP = w_0 \cdot \frac{\theta}{2}$ (half beam waist diameter w_0 times half far field divergence angle $\theta/2$)

$$BPP_{total} = \sqrt{BPP_{slow}^2 + BPP_{fast}^2} \leq BPP_{fiber} = \frac{d_{fiber}}{2} \cdot NA \quad (1)$$

Where d_{fiber} represents the optical fiber diameter and NA its numerical aperture.

In coupling diode laser power into fiber, the symmetry geometry of the fiber core makes highly desirable to have symmetrical BPPs at the fiber input surface. The symmetrization of the BPPs is equivalent to a minimization of the overall total beam parameter product BPP_{total} as it can be noticed in Eq. (1) [31- 35]. Due to the highly asymmetric output beam profile of the laser radiation from the diode laser bar, its BPP is greater than that of the optical fiber (Eq.1). To guarantee an efficient fiber coupling: $BPP_{total} < BPP_{fiber}$, it is only possible if the symmetrization of BPPs in both axes is achieved.

The beam shaping of a JOLD-50-CPBN-1L and the coupling of the output beam into a fiber are simulated using ZEMAX[®] ray tracing software that operates in a non-sequential mode. The non-imaging solution is based on the symmetrization of the diode laser radiation by means of two identical micro step-mirrors. Each single mirror surface of the first micro step-mirror is tilted 45° about the slow axis and separated from the neighbouring surface by a constant distance d along the axis of propagation (figure 2). The laser beam is incident on the first micro step-mirror. Here, it is cut into 13 sub-beams along the slow axis direction. Each sub-beam is reflected along the fast axis direction towards the second micro step-mirror, leading to sub-beams reflection into the slow-direction. In order to decrease the spot size on the fast axis, an anamorphic prism pair is used, which spatially compresses the spot height to 1/3 of its initial value. The BPP resulting from this beam shaping technique along the slow axis is 21.3mm.mrad whereas along the fast axis is 8.5mm.mrad.

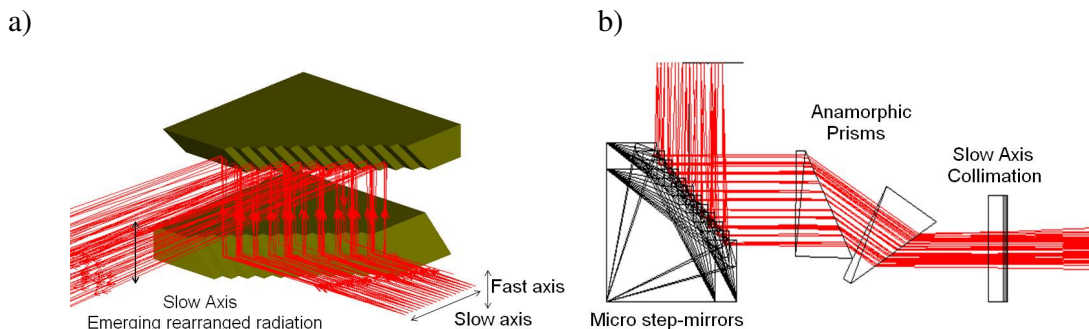


Figure 2. a) Realization of beam rearranging by a pair of step-mirrors consisting of 13 steps. b) Top side view of the compression unit.

To increase the output power of the system with a single diode bar, the emission of two diode laser bars are combined by using the polarization multiplexing technique. This way, the power of the system can be increased to twice of the original, whereas the beam quality would not be influenced. As it will be described in section 4.1, the light from JOLD-50-CPBN-1L diode bar has been analyzed and was obtained that it has a TE-polarization 97%. The direction of polarization of both diode laser bars is parallel to the slow axis. Therefore, polarization rotation of one bar using a $\lambda/2$ wave-plate is required to allow the overlapping of the emission from both diode bars, which has been done by a polarization beam splitter (PBS) (figure 3).

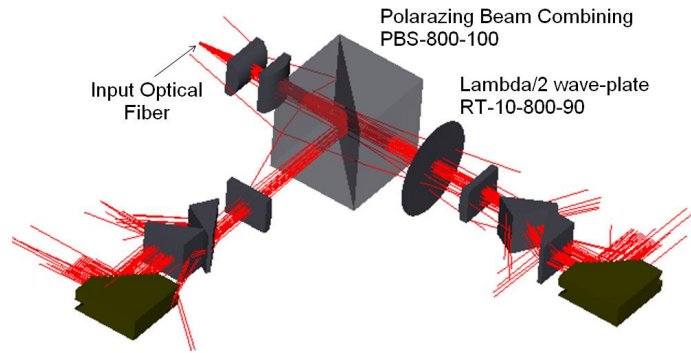


Figure 3. Ray tracing of the arrangement of two JOLD-50-CPBN-1L fiber coupling.

4. EXPERIMENTAL AND DISCUSSION

4.1 Polarization analysis

The diode laser bars (JOLD-50-CPBN-1L) are TE-polarized, i.e., the main component of the electric field vector is parallel to the heterointerfaces. The degree of polarization (DoP) was measured in order to predict the power losses associated with polarizing components used in the optical system. The DoP is a measure of the randomness of polarization in a light beam [35] and can be described by the following equation:

$$DoP(TE) = \frac{\overline{I_x} - \overline{I_z}}{\overline{I_x} + \overline{I_z}} \quad (2)$$

Where $\overline{I_x}$ represents the laser beam intensity measured in the plane of the junction (TE) and corresponds to the average value of the two intensities measured at polarization angles of 0° and 180° ; $\overline{I_z}$ the intensity measured in the perpendicular plane and corresponds to the average value of the two intensities measured at polarization angles of 90° and 270° . So that, a DoP of -1 means 100% TM polarization while a DoP of 1.0 means 100% TE polarization. A DoP of 0 indicates either equal components of each polarization are present or complete random polarization [36-37]. The DoP analysis was carried out by considering a polarizer (GL10-B, Thorlabs) located between the diode bar and the thermopile. The polarizer was rotated through 360° while the polarization of the bar was measured. Figure 4 shows the system polarization graphed on a polar plot, indicating that the diode laser bar is primarily polarized in the plane of the junction corresponding to TE polarization. The DoP=0.97 reveals that, when coupling the two diode laser bars, considering a proper beam alignment, about 3% of the laser power will be lost when the incident beam passes through the polarizing beam splitter (PBS).

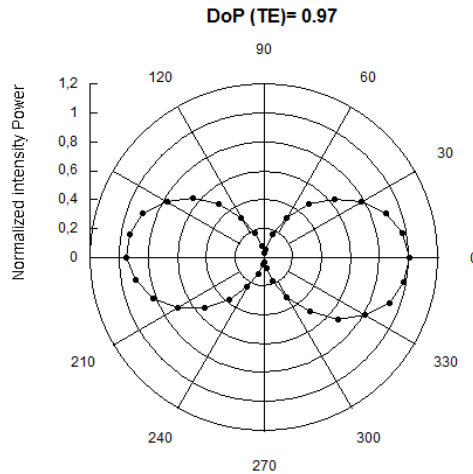


Figure 4. Polarization plot of a JOLD-50-CPBN-1L at 5W of laser power emission.

4.2 Beam shaping and fiber coupling

Considering the emission properties of the JOLD-50-CPBN-1L behind the collimation microoptics, the asymmetric radiation provides a $BPP_{\text{slow}} \sim 174\text{mm}$ and $BPP_{\text{fast}} \sim 0.002\text{mm}$. As it was stressed earlier, laser beam shaping is needed to guarantee an efficient fiber coupling ($BPP_{\text{laser beam}} < BPP_{\text{fiber}}$). Experiments were performed using with $600\mu\text{m}$ and $400\mu\text{m}$ fibers. The numerical aperture of both fibers is 0.22. According to equation 1, their corresponding BPP are 66.5 and 48.8mm.mrad respectively.

Once the beam has been shaped, i.e. the BPP has been equalized, to reach an efficient fiber coupling; the intensity distribution of the two laser beams has been analyzed by the ZEMAX[®] model, as well as experimentally (figure 5). Figure 5a shows the intensity distribution of the two laser beams emerging from the micro-step mirrors obtained by the the ZEMAX model and figure 5b the corresponding experimental far-field measurement [Primes Beam Monitor BM60 4623]. The laser beams are not showed overlapped due to the overlapping between laser beams is produced on the last stage of rearrangement laser beams. As it can be seen, the intensity distribution emerging from each micro-step mirror systems consists of ten stripes coming from the reflection from the individual steps of the mirror pair [20, 26]. Their intensity distribution broadens from left to right side. This effect can be caused by the staircase-like displacement of each micro-mirror along the axis of propagation. Furthermore, the left and the right stripes of each laser beam exhibit a cut-off, which can be originated from the fact that the outer mirrors are not illuminated by the full slow-axis angle of the light cone of the diode laser [26].

The figure 6 shows the simulated and measured intensity distribution of the far field laser beam behind the last stage of rearrangement: micro-steps mirrors + anamorphic prism pair + slow axis collimation lens. It can be observed that the cross sections of the laser beams have similar dimensions in fast and slow axis, which mean that a symmetrization of the laser beam has been achieved. In both cases, figure 5 and 6 the experimental results were well – reproduced by the ZEMAX[®] model. The slight deviations observed in a qualitative comparative analysis can be due to different relevant reasons:

- The ZEMAX[®] model assumes an equal intensity distribution for every diode laser emitter of the diode bar (19) for near and far field distribution. This assumption is not strictly true since the laser beam power at the corners is lower than that at the center [33].
- The intensity distribution of each diode laser can be improved by means of the calibration of the spatial super-Gaussian factor of the diode laser emitters [38].
- In the ZEMAX[®] model has not been taken into account possible effects of smile. This effect occurs if some emitting facets of the diode laser bar are displaced by a small distance of only μm from a straight line along the

slow axis. Due to the short focal length of the diode bar micro-lens this has a significant effect on the divergence angle after them. [26-27].

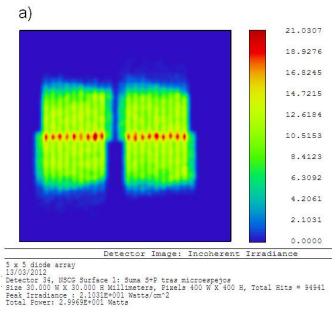


Figure 5. a) Simulated and b) experimental far field irradiance of the reshape laser beam after the micro-step mirrors at 10W of laser power emission. Vertical: Slow Axis, Horizontal: Fast axis.

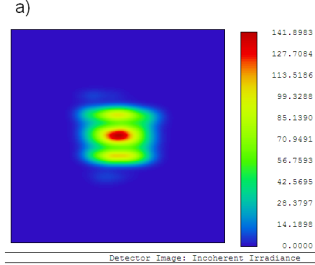
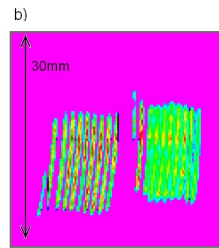
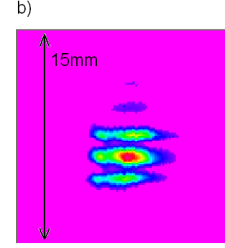


Figure 6. a) Simulated and b) experimental irradiance of the collimated laser beam at 10W of laser power emission. Vertical: Slow Axis, Horizontal: Fast axis.



Therefore, by means of this technique it has been possible to reshape the rectangular output beam from two diode laser bar into a square laser beam with similar beam quality in both axes lower than the selected fiber BPP (figure 6).

Finally, the reshaped laser beam is focused and coupled to the optical fiber, achieving a high quality and high efficiency fiber coupled diode laser system. The slow and fast directions of the collimated laser beam are focused by means of two cylindrical lenses, with focal lengths of 15 and 20mm, respectively. A measurement of the beam quality of the laser system is shown in figure 7a). The beam quality was characterized [Coherent Beam Master BM-7 PCI 2968] by a BPP of 39.1mm.mrad and 27.3mm.mrad for the slow and fast directions, respectively. Consequently, the diagonal BPP of the laser beam is about 47.7mm.mrad

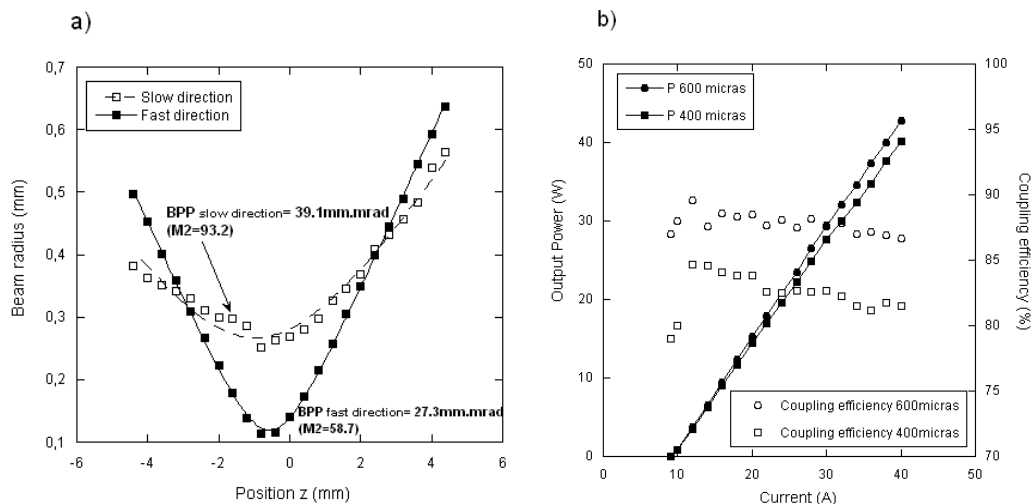


Figure 7. a) Beam quality measurement of the laser system at 6W of laser power emission; b) Output power and coupling efficiency for a 600µm and 400µm fibers both with numerical aperture of 0.22.

The results in term of coupling efficiency and emission power for fiber coupling are shown in the figure 7b) with 600µm and 400µm NA.0.22 optical fibers. The power transmitted through the fiber was measured with a thermopile. Maximum output power at 40A was 43W for 600µm and 40W for the 400µm fiber. The corresponding coupling efficiencies were 87% and 81% respectively. As it can be expected, the coupling efficiency of the 600µm is higher than that achieved with a 400µm fiber, due to the large extent of the spot breaches the dimension of the 400µm fiber. Furthermore, it can be seen

that, in both cases, the coupling efficiency decreases with increasing injection current. This fact can be due to the decrease of the beam quality when increasing the operant current. The slow-axis divergence increases with increasing injection current [20, 39]. Although this effect is not drastic, it broadens the dimensions of the focus spot and thus, decreases the coupling efficiency slightly.

Having into account all the losses in the system, the overall efficiency of the presented high-power diode laser optical fiber coupled system is about 67% and 61% for the 600 μ m and 400 μ m optical fibers respectively. Before fiber coupling, After the laser beam has passed through the beam shaping optics (figure 3), the energy losses are around 20%. This transfer energy is strongly influenced by the micro-step mirrors and the polarization beam splitter (PBS) in which the relative energy lost is about 15% and 5% respectively. The latter is match up the obtained degree of polarization (DoP) of the diode laser bar (figure 3).

4.3 Laser transmission welding

The weld seams are assessed by three different means including: visual inspection, appearance optical micrographs of the weld seams and weld tensile force at failure. Following the results corresponding to these three assessments will be shown. As it had been described above, all these welded seams were cross sectioned in order to carry out a microscopic inspection of their integrity. The figure 8 illustrates the image of an a) weld seam with pores trapped in centre of weld, b) good welding result without pores or decomposed material and c) a degraded joint. By visual inspection of the optical micrographs, a good quality weld seam (figure 8b) is considered along the melting layer when there is no evidence neither pores nor polymer degradation. In these cases, the weld width seam is measured between the edges of the heat affected zone.

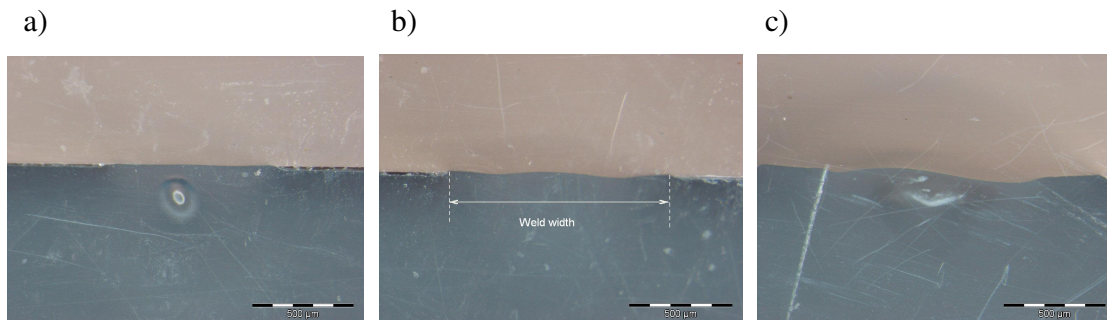


Figure 8. Optical micrographs of a representative a) poor joint P=6W b) optimal joint P=8.5W c) degraded joint done with P=16.5W in the case of ABS/ABS-0.01%CNT at v=15mm/s.

In the figure 9a) are plotted the optimum welded seams for both percentages of CNTs versus line energy, which is directly proportional to the laser power and inversely varies with the welding speed. Consequently, for a certain welding speed, at higher laser powers shown burn appearance and at lower powers it shown the appearance of pores. Considering all the trials, the standard deviation provide by the replications of each trial ranging between 0.2% and 8% for both concentration of CNTs.

For both percentages of CNTs, the figure 9 shows that at higher line energy the weld width tend to attain a maximum. Further increase of line energy does not increase the weld width.

On the one hand, the results regarding the behavior of the weld width depending on the welding speed are analyzed. In the case of ABS/ABS-0.01%CNT they suggest that the increase power needed in order to keep the same value of line energy by the fact of increasing the welding speed has not remarkable effect on the weld width. However, the results corresponding on the case of ABS/ABS-0.05%CNT indicate that the increases required power show a moderate influence on the weld width: for the same line energy value bigger weld width are achieved at higher laser powers. Consequently, these results suggest that the higher percentage of CNTs the higher sensitivity to laser power changes. Besides, this tend can explain the bigger processing window for creating a high quality welded seam in the case of ABS/ABS-0.01%CNT with respect to ABS/ABS-0.05%CNT.

On the other hand, the same value of weld width can be achieved by means of different laser powers at the same welding speed depending on the used percentage of CNTs. To illustrate, at 15mm/s welding speed a weld width of 1mm can be achieved at 4.2W in the case of ABS/ABS-0.05%CNT and 8W are needed in the case of ABS/ABS-0.01%CNT. This result could be explained in base on the optical properties of both additive polymers.

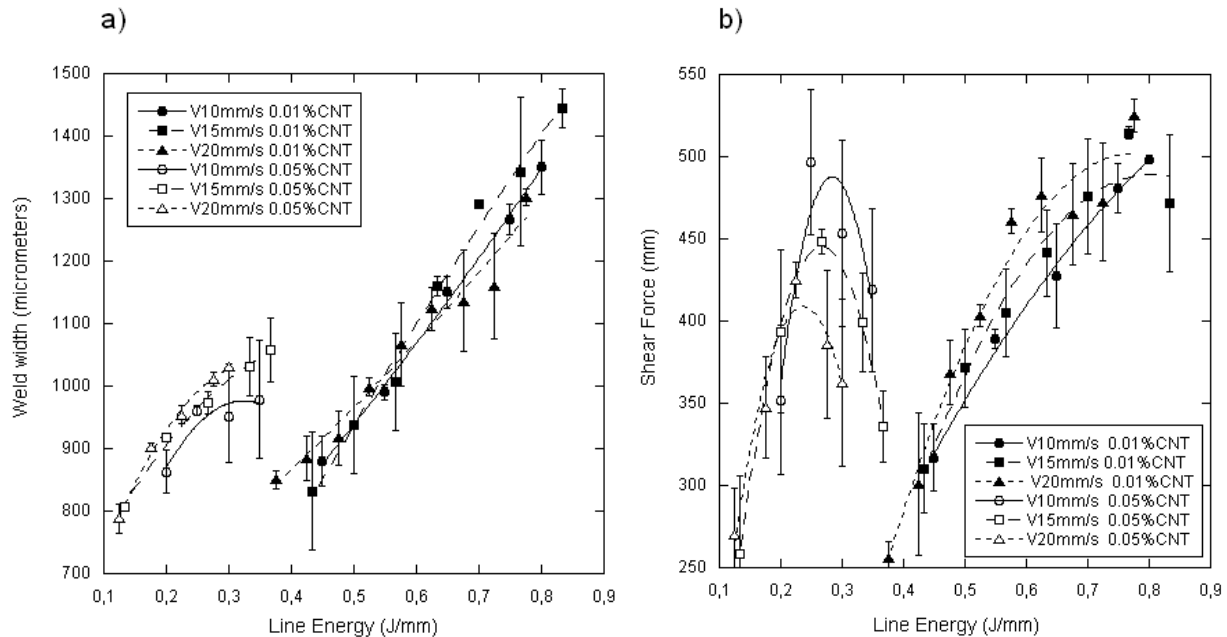


Figure 9. Average a) weld width b) shear force as a function of line energy for two different percentages of CNTs.

Regarding the mechanical testing, the ABS/ABS-CNT joints were subjected to a destructive test in order to know their mechanical resistance. The shear forces were recorded as the force at which the joint broke into separate pieces. The figure 9b) reports the average measured shear force for each welding trial shown in figure 9a). The standard deviations of all shear force values are located between 0.5% and 14% of the average value.

Firstly, the dependency of the shear force with the process parameters in the case of ABS/ABS-0.01%CNT is analyzed. Taking into account the error bars showed, the influence of the power increase on the shear force at certain line energy can be neglect. In addition to this, one can appreciate that the maximum value of the shear force for each welding speed is located at around the same line energy value at which the maximum weld width was found (figure 9a)). The latter is in agreement with to suppose a slight sensitivity of the polymer response at changes in the laser power keeping the same value of line energy.

In the case of ABS/ABS-0.05%CNT it can be see that the higher welding speed the lower shear force for the same line energy value. It involves that, although the behavior of the weld width is opposite, the weld seam quality is worse as consequence of the higher power density along with the high sensitivity of the ABS/ABS-0.05%CNT by changing laser power. Base on this sensitivity, it is possible to explain the displacement of the maximum value of shear force with respect to the maximum weld width found for each welding speed (figure 9a).

5. CONCLUSIONS

In this paper, we have reported the modeling of a diode laser system using ZEMAX[®] ray tracing software and its subsequent validation. A study of laser weldability of ABS filled with two different concentrations of CNTs has been carried out using the presented high-power diode-laser optical fiber coupled system.

The ray tracing software ZEMAX[®] represents a powerful tool to model optical systems which are going to be implanted in an industrial sector. The ZEMAX[®] model solution and experimental results showed good agreement. Coupling into a 600 μ m and 400 μ m fiber have been performed in 87% and 81% respectively, leading to a power efficiency of the system of 67% and 61% for 600 μ m and 400 μ m respectively.

The required laser power to reach an optimum weld seam on ABS is directly related to the concentration of the CNTs in the polymer matrix. According to this, there is a direct relationship between optical properties of the polymer and welding process parameter: ABS/ABS-0.01%CNT plates are less sensitive to laser power changes than in the case of ABS/ABS-0.05%CNT, providing smaller weld width at higher welding speeds. This results leads to a wider processing window for ABS with low concentration of carbon nanotubes.

REFERENCES

- [1] Amanat, N., James, N.L., McKenzie, D.R., "Welding methods for joining thermoplastics polymers for the hermetic enclosure of medical device", *Medical engineering and Physics* 32, 690-699 (2010).
- [2] Tsao CW, DeVoe DL. "Bonding of thermoplastic polymer microfluidics". *Microfluid Nanofluid* 6, 1–16 (2009).
- [3] Becker, H., Gartner, C., "Polymer microfabrication technologies for microfluidic Systems". *Analytical and Bioanalytical Chemistry* 390, 89–111 (2008).
- [4] M. Kalpana, "Plastics Welding Technology for Industry", *Assembly Automation*, 17-3, 196-200, (1997).
- [5] Velten, T., Ruf, H.H., Barrow, D., Aspragathos, N., Lazarou, P., Jung, E., et al. "Packaging of bio-MEMS: strategies, technologies, and applications". *IEEE Transactions on Advanced Packaging* 28, 533–46 (2005).
- [6] Tsao, CW., DeVoe, DL., "Bonding of thermoplastic polymer microfluidics. *Microfluidics and Nanofluidics* 6, 1–16 (2009).
- [7] Ageorges, C., Ye L, Hou M. "Advances in fusion bonding techniques for joining thermoplastic matrix composites: a review". *Composites Part A: Applied Science and Manufacturing* 32, 839–57 (2001).
- [8] Potente, H., Karger, O., Fiegler, G., "Laser and microwave welding – the applicability of new process principles". *Macromol Mater Eng* 87, 734–44 (2002).
- [9] Tsao, CW., DeVoe, D.L., "Bonding of thermoplastic polymer microfluidics. *Microfluidics and Nanofluidics* 6, 1–16 (2009).
- [10] Amanat, N.C., Chaminade, Grace, J., McKenzie, D.R., James, N.L., "Transmission laser welding of amorphous and semi-crystalline poly-ether-ether-ketone for applications in the medical device industry". *Materials and Design* 31, 4823-4830 (2010).
- [11] Visco, A.M., Campo, N., Torrisi, L., Caridi, F., "Effect of carbon nanotube amount on polyethylene welding process induced by laser source" *Applied physics A: materials science & processing*, 103(2) 439-445 (2011).
- [12] Coelho, J.P., Abreu, M.A., Pires, M.C., "High-speed laser welding of plastic films" *Opt. Lasers Eng.* 34, 385 (2000).
- [13] Boglea, A., Olowinsky A., Gillner A., "Fibre laser welding for packaging of disposable polymeric microfluidic-biochips". *Appl. Surf. Sci.* 254, 1174–8 (2007).
- [14] Ulrich A. Russek, A. Palmen, H. Staub, J. Poehler, C. Wenzlau, G. Otto, M. Poggel, A. Koeppel and H. Kind, "Laser beam welding of thermoplastics", *Proc. SPIE* 4977, 458-472 (2003).
- [15] Van de Ven, J.D., Erdman, A.G., "Laser transmission welding of Thermoplastics- Part II: Experimental Model Validation", *Journal of Manufacturing Science and Engineering*, 129, 859-867, (2007).
- [16] Becker, F., Potente, H., "A step Towards Understanding the Heating Phase of Laser Transmission Welding in Polymers", *Polymer Engineering and Science*, 42, 365-372 (2002).
- [17] Ghorbel, E., Casalino, G., Abed S., "Laser diode transmission welding of polypropylene: Geometrical and microstructure characterization of weld", *Material and Design*, 30 (7), 2745-2751 (2009).
- [18] Seyed Hamed Ghasemi, Mohammad-Reza Hantehzadeh, Jamshid Sabbaghzadeh, Davoud Dorrani, Majid Lafooti, Vahid Vatani, Reza Rezaei-Nasirabad, Atefeh Hemmati, Ali Asghar Amidian, and Seyed Ali Alavian, "Beam shaping design for coupling high power diode laser stack to fiber," *Appl. Opt.* 50, 2927-2930 (2011)
- [19] Wang, Z., Segref, A., Koenning, T., and Pandey, R., "Fiber coupled diode laser beam parameter product calculation and rules for optimized design", *Proc. SPIE* 7918, 791809 (2011);
- [20] Heinemann, S. and Leininger, L., "Fiber-coupled diode lasers and beam-shaped high-power stacks", *Proc. SPIE* 3267, 116-124 (1998).

- [21] Schreiber, P., Hofer B., Dannberg, P., and Uwe D. Zeitner, "High-brightness fiber-coupling schemes for diode laser bars", Proc. SPIE 5876, 587602 (2005)
- [22] Zbinden, H., and Balmer, J.E., "Q-switched Nd:YLF laser end pumped by a diode-laser bar" Opt. Lett. 15, 1014 (1990)
- [23] Graf, Th. and Balmer, J.E., "High-power Nd:YLF laser bar end pumped by a diode-laser bar" Opt. Lett. 18, 1317 (1993)
- [24] Yamaguchi, S., Kobayashi, T., Saito, Y., and Chiba, K. "Collimation of emissions from a 1-cm aperture tightly arranged, multistripe laser-diode bar with a multiprism array coupling," Appl. Opt. 36, 1875-1878 (1997)".
- [25] Clarkson, W.A., and Hanna, D. C., "Two-mirror beam-shaping technique for high-power diode bars," Opt. Lett. 21, 375-377 (1996)
- [26] Ehlers B., Du, K., Baumann, M., Treusch, H.G., Loosen, P. and Poprawe, R., "Beam shaping and fiber coupling of high-power diode laser arrays", Proc. SPIE 3097, 639-644 (1997).
- [27] Diehl, R., [High-Power Diode Lasers Fundamentals, Technology, Applications], Springer, 303-331 2000
- [28] Koening, T., Alegria, K., Wang, Z., Segref, A., Stapleton, D., Faßbender, W., Flament, M., Rotter, K., Noeske, A. and Biesenbach, J, "Macro-channel cooled high power fiber coupled diode lasers exceeding 1.2kW of output power", Proc. SPIE 7918, 79180E (2011).
- [29] <http://www.jenoptik.com/>
- [30] Sokolowski, W., Wolff, D., and Hennig, P., "Beam shaping and fiber coupling of high power diode lasers", Proc. Of the Symposium on Photonics Technologies for 7th Framework Program, 129-132 (2006).
- [31] Schreiber, P., Hofer, B., Dannberg, P., Zeitner, U.D., "High-brightness fiber-coupling schemes for diode laser bars", Proc. SPIE 5876, 587602 (2005).
- [32] Köhler, B., Ahlert, S., Branda, T., Haaga, M., Kissel, H., Seibold, G., Stoiber, M., Biesenbach, J., Reill, W., Grönninger, G., Reufer, M., König, H., Strauss, U., "Diode laser modules base on new developments in tapered and broad area diode laser bars", Proc. of SPIE 6876 (2008).
- [33] Koening, T., Alegria, K., Wang, Z., Segref, A., Stapleton, D., Faßbender, W., Flament, M., Rotter, K., Noeske, A. and Biesenbach, J, "Macro-channel cooled high power fiber coupled diode lasers exceeding 1.2kW of output power", Proc. SPIE 7918, (2011).
- [34] Zuolan Wang, Z., Segref, A., Koening, T., and Pandey, R., "Fiber Coupled Diode Laser Beam Parameter Product Calculation and Rules for Optimized Desing", Proc. SPIE 7918-13,(2011).
- [35] Wessling, C., Hengesbach, St., Geiger, J, Dolkemeyer, J., Traub, M., Hoffmann, D., "50W passively cooled, fiber coupled diode laser at 976 nm for pumping fiber lasers using 100 µm fiber bundles", Proc. SPIE 6876, 687614 (2008)
- [36] Bass, M., [Handbook of Optics: Vol.I- Geometrical and physical optics, polarized light, components and instruments], Mc Graw Hill, Third Edition 484-488 (2010)
- [37] Hostetler, J.L., Jiang, C.-L., Negoita, V., Vethake, T., Roff, R., Shroff, A., Li, T., Miester, C., Bonna, U., Charache, G., Schlüter, H., and Dorsch, F., "Thermal and strain characteristics of high-power 940 nm laser arrays mounted with AuSn and In solders", Proc. SPIE 6456, 645602 (2007).
- [38] Coluccelli, N., "Nonsequential modeling of laser diode stacks using Zemax: simulation, optimization, and experimental validation", Applied Optics 49(22), 4237-4245 (2010).
- [39] Koehler, B., Biesenbach, J., Brand, T., Haag, M., Huke, S., Noeske, A., Seibold, G., Behringer, M., and Luft, J., "High-brightness high-power kW system with tapered diode laser bars", Proc. SPIE 5711, 73 (2005).